Biobased Polyurethanes from Polyether Polyols Obtained by Ionic-Coordinative Polymerization of Epoxidized Methyl Oleate

E. DEL RIO, G. LLIGADAS, J. C. RONDA, M. GALIÁ, V. CÁDIZ

Departament de Química Analítica i Química Orgánica, Universitat Rovira i Virgili, Campus Sescelades, Marcel.lı´ Domingo s/n, 43007 Tarragona, Spain

ABSTRACT: A series of poly(ether urethane) networks were synthesized from polyether polyols obtained by ionic-coordinative polymerization of epoxidized methyl oleate (EMO) using 4,4′-methylenebis(phenyl isocyanate) or L-lysine diisocyanate as coupling agents. Moreover, a variety of segmented poly(ether urethane) networks with different hard segment contents were obtained using 1,3-propanediol as the chain extender. The materials were characterized by differential scanning calorimetry, thermogravimetric analysis, dynamic mechanical thermal analysis, and tensile properties.

KEYWORDS: biopolymers; polyols; polyurethanes; renewable resources

INTRODUCTION

Recent years have witnessed an increasing demand on natural products in industrial applications for environmental issues, waste disposal, and depletion of nonrenewable resources.[1] Renewable resources can provide an interesting sustainable platform to substitute petroleumbased polymers through the design of bio-based polymers that can compete or even surpass the existing materials on a cost–performance basis with high eco-friendliness values.[2,3] Plant oils are considered as the most important renewable raw materials for the production of bio-based polymers. In recent years, a variety of polymeric materials have been developed and tested with plant oils as feedstock.[4–7]

Polyurethanes are one of the most important and versatile materials with applications ranging from flexible foams in upholstered furniture to rigid foams as insulators in walls, roofs, and appliances of thermoplastic polyurethanes used in medical devices and footwear, coatings, adhesives, sealants, and elastomers used on floors and automotive interiors.[8] They represent an important class of thermoplastic and thermosets because their mechanical, thermal, and chemical properties can be tailored by reactions with various polyols and isocyanates. Usually, both isocyanates and polyols are petroleum based, but, in recent years, vegetable oils, fatty acids, and their derivatives have attracted significant attention as raw materials for the preparation of polyurethanes.[9]

For natural oils to be used as raw materials for polyol production, multiple hydroxyl functionality is required. Different ways of preparing vegetable oil-based polyols have been successfully developed: epoxidation and further oxirane ring opening,[10,11] hydroformylation,[12] ozonolysis,[13] or reaction at the double bonds and subsequent reduction of the carboxyl groups that yields polyethers containing the hydroxyl groups.[14] However, limited attention has been paid to the preparation of polyether polyols from vegetable oils. Polyether polyols with molecular weights of 200–10,000 g/mol are important building blocks for polyurethane applications.[15] Polyols with molecular weights of about 3000 or more are used to produce flexible polyurethanes, and polyols of about 200–1200 g/mol are used for rigid polyurethanes. Polyether polyols are usually produced by the anionic ringopening polymerization of alkylene oxides such as ethylene oxide or propylene oxide.

To further extend the applications of vegetable oils, our group has focused on converting these renewable resources into useful biopolymers. In a previous study, we described the synthesis of polyether polyols through the combination of cationic ring-opening polymerization of epoxidized methyl oleate (EMO) and the reduction of carboxylate groups to hydroxyl moieties. Polyols with different hydroxyl contents were obtained and reacted with 4,4′-methylenebis(phenyl isocyanate) (MDI) to yield polyurethanes that behave like hard rubbers or rigid plastics.[14] A series of biodegradable segmented poly(ether urethane) networks were obtained from the EMO based polyether polyol and 1,3-propanediol (PDO) using L-lysine diisocyanate (LDI) as a nontoxic coupling agent.[16] We have also developed novel biobased silicon-containing polyurethanes from these polyols and a silicon-containing polyol with terminal primary hydroxyl groups.[17]

TABLE 1 General Properties of the Obtained Polyols

Polyol	Millimoles $LiAlH_4$ per Gram of Polymer	OH[a] (wt %)	Reduction Degree (%)	M_n (SEC)	M_w/M_n	Functionality[b]	EW (g/equivalent)[c]
POH11	0.24	0.66	11	7100	1.6	2.4	2960
POH15	0.3	0.88	15	6700	1.7	3.5	1914
POH20	0.4	1.19	20	6600	1.7	4.6	1440
POH28	0.55	1.67	28	6700	1.7	5.8	1140
POH40	0.8	2.39	40	6600	1.7	9.3	710

[a] Hydroxyl content values from ^1H and ^{19}F NMR.
[b] Functionality was obtained by dividing the experimental molecular weight (M_n) by the hydroxyl content.
[c] Equivalent weight calculated by dividing the experimental molecular weight (M_n) by the functionality.

Long-chain internal oxiranes or functionalized epoxides show low reactivity because of a higher sterical hindrance and side reactions, and high-molecular-weight polymers cannot be obtained by using anionic or cationic catalysts.[18] We obtained oligomeric polyethers of about 900–1200 g/mol through the acid-catalyzed ring-opening polymerization of EMO.[14] Coordinative ring-opening polymerization has been described for functionalized epoxides as phenylglycidylether derivatives[19] or ω-epoxy alkanoates.[20] In a previous study, we developed new polyether polyols by ioniccoordinative polymerization of EMO with molecular weights around 7000 g/mol.[21] This work seeks to broaden the physical properties of vegetable oil-based polyurethanes by using these polyethers, thus increasing the molecular weight of the polyol. Polyols were obtained by the controlled reduction of the carboxylate groups to hydroxyl moieties using lithium aluminum hydride as reducing agent and were characterized by chemical methods, spectroscopic (Fourier transform infra red [FTIR] and nuclear magnetic resonance [NMR]), and thermal (differential scanning calorimetry [DSC]) techniques. They were reacted with PDO and MDI or LDI to obtain polyurethane networks with various hard segment contents. The properties of prepared polyurethanes were studied by using DSC, thermogravimetric analysis (TGA), and dynamic mechanical thermal analysis (DMTA).

EXPERIMENTAL

Materials

Methyl oleate 90plusV_R was kindly supplied by T+T Oleochemie. EMO was synthesized using a literature procedure.[22] EMO-based polyether was synthesized in our laboratory using the procedure described earlier (M_n = 6400 M_w/M_n = 1.7).[21]

The following chemicals were obtained from the sources indicated and used as received: lithium aluminum hydride (Aldrich), MDI (Aldrich), and 2,6-diisocyanato methyl caproate (L-lysine diisocyanate, LDI) (Kyowa Hakko Kogyo Co.). Chain extender, PDO, was purchased from Aldrich and was distilled and stored at ambient temperature in a dessicator until used. Tetrahydrofuran (THF) was distilled from sodium-benzophenone immediately before use. Other solvents were purified by standard procedures.

Representative Procedure for the Reduction of Polyether PEMO

In a round bottom flask, 5.95 g of PEMO (19.0 mmol) was dissolved in 150 mL of freshly anhydrous THF under argon atmosphere and vigorous stirring. The desired amount of $LiAlH_4$ was added in small portions, and, after addition was complete, the mixture was stirred vigorously at room temperature for 30 min. Traces of unreacted $LiAlH_4$ were decomposed by addition of 5 mL ethyl acetate dropwise. Then, a 10% H_2SO_4 aqueous solution was slowly added. The phases were separated, and the aqueous layer was extracted with ethyl acetate. The combined organic phases were washed with H_2O, saturated $NaHCO_3$ solution, and saturated NaCl solution, dried over anhydrous magnesium sulfate, and the solvent removed in vacuo. The polymers were dried at 50 °C under vacuum for 24 h (see Table 1 for general properties).

^{1}H-NMR ($CDCl_3$, tetramethylsilane [TMS], δ in ppm): 3.63 (s, -O-CH_3), 3.65–3.55 (t, -CH_2OH), 3.40–3.10 (m, polyether backbone), 2.27 (t, -CH_2-CO_2Me), 1.70–1.10 (m, -CH_2-aliphatic backbone), 0.85 (t, -CH_3). ^{13}C NMR ($CDCl_3$, TMS, δ in ppm): 174.3 (-CO_2Me), 82–74 (polyether backbone), 62.9 (-CH_2OH), 51.6 (-OMe), 34.2 (-CH_2CO_2Me), 32.9 (-CH_2-CH_2OH), 32.1 (-CH_2-CH_2-CH_3), 31–25.5 (m, aliphatic backbone), 25.2 (-CH_2-CH_2-CO_2Me), 22.9 (-CH_2-CH_3) 14.3 (-CH_3).

Representative Procedure for the Synthesis of Polyurethanes

Polyurethanes were synthesized by reacting the appropriate amount of polyol and 1,3-propandiol for the segmented polyurethanes with a 2% molar excess of the isocyanate (MDI or LDI). Samples were prepared by vigorous stirring of the reactants at 60 °C under argon, and the mixture was poured into a mold (5 cm length and 0.6 cm width) and degassed under vacuum. Mixtures were cured under argon atmosphere as follows: Polyurethanes derived from MDI (PUM) at 60 °C for 2 h and 110 °C for 12 h. Polyurethanes derived from LDI (PUL) at 90 °C for 2 h and 110 °C for 12 h. Segmented polyurethanes derived from MDI (SPUM) at 70 °C for 12 h and 130 °C for 2 h. Segmented polyurethanes derived from LDI (SPUL) at 110 °C for 12 h and 130 °C for 2 h. Chemical composition and hard segment content of the polyurethanes are shown in Table 2.

TABLE 2 Chemical Composition of the Polyurethanes

Sample Code	Polyol	Isocyanate	Molar Composition[a]	%HS[b]
PUM11	POH11	MDI	1.00/0.00/1.02	–
PUM15	POH15			–
PUM20	POH20			–
PUM28	POH28			–
PUM40	POH40			–
PUL11	POH11	LDI	1.00/0.00/1.02	–
PUL15	POH15			–
PUL20	POH20			–
PUL28	POH28			–
PUL40	POH40			–
SPUM15	POH20	MDI	1.00/1.78/2.83	15
SPUM34			1.00/5.24/6.36	34
SPUM47			1.00/9.04/10.24	47
SPUL15	POH20	LDI	1.00/2.14/3.16	15
SPUL34			1.00/5.66/6.79	34
SPUL47			1.00/10.57/11.80	47

[a] mol OH Polyol:mol OH PDO:mol isocyanate.
[b] % Hard segment calculated as weight percentage of PDO and isocyanate per total material weight.

CHARACTERIZATION

^{1}H NMR (400 MHz), ^{13}C NMR (100.6 MHz) and ^{19}F NMR (376.4 MHz) spectra were recorded in $CDCl_3$ using a Varian Gemini 400 spectrometer. Chemical shifts were reported in ppm relative to TMS, $CHCl_3$, and $CFCl_3$ as internal standards. The IR spectra were recorded on a Bomem Michelson MB 100 FTIR spectrophotometer with a resolution of 4 cm^{-1} in the absorbance mode. An attenuated total reflection accessory with thermal control and a diamond crystal (Golden Gate heated single-reflection diamond ATR, Specac-Teknokroma) was used to determine FTIR spectra.

Calorimetric studies were carried out on a Mettler DSC822e thermal analyzer using N_2 as a purge gas (20 mL/min) at a scan rate of 20 ^{o}C/min. Thermal stability studies were carried out on a Mettler TGA/SDTA851e/LF/1100 with N_2 or synthetic air as purge gases. The studies were performed in the 30–800 ^{o}C temperature range at a heating rate of 10 ^{o}C/min.

Size exclusion chromatography analysis was carried out with an Agilent 1200 series system with PLgel 3 µm MIXED-E, PLgel 5 µm MIXED-D, and PLgel 20 µm MIXED-A columns in series, and equipped with an Agilent 1100 series refractiveindex detector. Calibration curves were based on polystyrene standards having low polydispersities. THF was used as an eluent at a flow rate of 1.0 mL/min, the sample concentrations were 5–10 mg/mL, and injection volumes of 100 µL were used.

The mechanical properties were measured with a TA DMA 2928 dynamic mechanical thermal analyzer. Specimens 2.0 mm thick, 5 mm wide, and 10 mm long were tested in a three-point-bending configuration. Temperature ranges from 100 ^{o}C to 150, 200, or 250 ^{o}C depending on polyurethane at a heating rate of 3 ^{o}C/min and at a fixed frequency of 1 Hz. Stress–strain curves were carried out by applying 0.1 N/min controlled force at 40 ^{o}C.

Hydroxyl Value Determination

The millimoles of hydroxy groups per gram of polymer were determined by ^{1}H NMR and ^{19}F NMR using 2-fenylethyl-trifluoroacetate as internal standard. The samples were derivatized with trifluoroacetic acid anhydride. Reactive hydroxyl groups were calculated as follows:

mmol of reactive OH per gram of POH = (mmol IS x Integral POH/Integral IS) / g POH

where POH is the reduced polymer, IS is the internal standard, mmol IS is the amount of internal standard added to the sample in millimoles and g P-OH is the quantity of sample measured in grams.

RESULTS AND DISCUSSION

Synthesis of Polyols

PEMO (M_n = 6400, M_w/M_n = 1.7)[21] was used as starting material for the partial reduction of the ester groups to synthesize polyols having primary hydroxyl moieties. The reduction was carried out with appropriate amounts of $LiAlH_4$ as reducing agent to obtain polyols having a 10, 15, 20, 30 and 40% of reduction degree (Table 1). We determined the hydroxyl content by ^1H- and ^{19}F NMR spectroscopy, and, as can be seen, polyols POH11, POH15, POH20, POH28, and POH40 showed reduction degrees very close to the expected. FTIR spectra of the polyols showed an increase in the hydroxyl groups' peak intensity (3500 cm^{-1}), whereas a decrease in the aliphatic ester carbonyl peak (1750 cm^{-1}) was observed. In the ^1H NMR spectra, a new signal appears at δ = 3.6 ppm due to the protons of the CH_2-OH moiety. As the reduction degree increases, the intensity of this signal increases, whereas the intensity of the peak at δ = 2.3 ppm, corresponding to the methylene attached to the ester group, decreases. In this way, polyols of similar molecular weight with a range of functionalities from 2.4 to 9.3 have been obtained, which are from clear to viscous liquids at room temperature. DSC traces for POH11 exhibit a broad melting peak centered at 20 °C, which shifts to higher temperatures when the hydroxyl content value increases. Moreover, a second melting endotherm can be observed at 0 C for POH40, with the highest functionality. Multiple peaks in these polyols should be ascribed to different crystalline forms.

Synthesis of Polyurethanes

Novel biobased polyurethanes were prepared from the abovementioned EMO-based polyether polyols and MDI or LDI. Moreover, segmented polyurethanes were prepared using POH20, MDI or LDI, and PDO as the chain extender using the one-shot technique, which consists of the very efficient mixing, in one step only, in a short time, of all the raw materials involved in polyurethane preparation: polyol, chain extender, and isocyanate. The chemical structure and the characteristics of the materials are shown in Scheme 1.

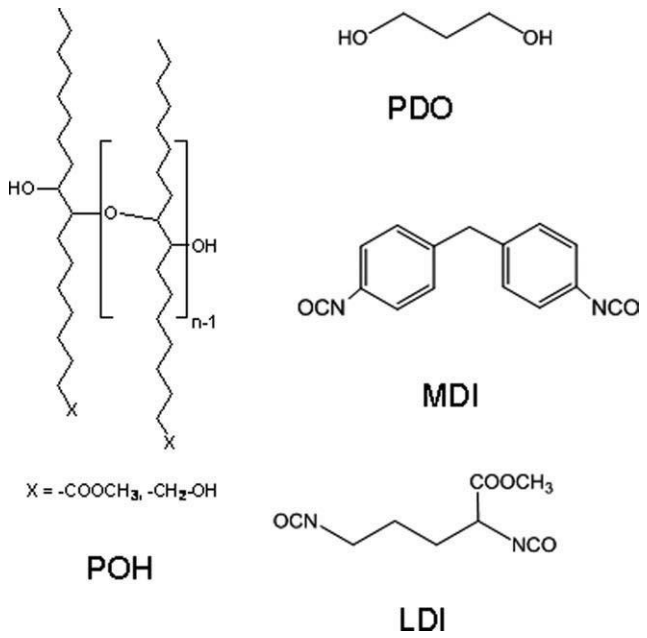

SCHEME 1 Chemical structure of polyols, PDO, MDI, and LDI.

The chemical composition and hard segment content of the synthesized polyurethanes are shown in Table 2. The NCO/OH molar ratio was kept constant at 1.02 to compensate for isocyanates that are consumed in side reactions during the urethane synthesis. For the segmented polyurethanes, the molar composition of the POH was set at 1.00, and then the molar ratio of the PDO and isocyanate were varied to obtain polyurethanes with different hard segment contents. For the MDIcontaining polyurethanes, reactants were mixed at 70 °C and cured at this temperature for 12 h before being postcured 2 h at 110 °C. The LDI-containing polyurethanes were obtained by curing 12 h at 110 °C and postcuring 2 h at 130 °C.

FTIR analysis demonstrated the urethane formation reaction during polymer synthesis. Figure 1 shows FTIR spectra before and after the curing of the polyurethane PUM28. The starting mixture shows a characteristic peak at 2240 cm^{-1} ascribed to -N=C=O stretching of the isocyanate moiety. During the curing, this peak significantly decreases and, after 2 h, completely disappears. The cross-linking reaction was

also monitored by the appearance of the characteristic absorbances of urethane link. The band due to the carbonyl stretching vibration of polyurethane occurs at 1723 cm^{-1}, overlapped with the C=O ester band, and a combination of N-H deformation as well as C-N stretching vibrations occurs at 1533 and 1233 cm^{-1}, respectively. Peak appearing at 1309 cm^{-1} is due to -OCONH asymmetric stretching vibrations. Moreover, the broad band centered at 3500 cm^{-1}, corresponding to the O-H stretching, shifts to lower frequencies, and shows a maximum at 3350 cm^{-1}, characteristic of N-H stretching.

FTIR spectroscopy was used to investigate the structural difference in hard and soft segments of synthesized polyurethanes with various PDO fractions. Almost all the infrared research on polyurethanes has focused on two principal vibrational regions: the N-H stretching vibration (3200–3500 cm^{-1}) and the carbonyl C=O stretching vibration amide-I region (1700–1730 cm^{-1}).[23,24] Polyurethanes are capable of forming several kinds of hydrogen bonds because of the presence of donor N-H group and C=O acceptor group in the urethane linkage. The oxygen atom of the ester or ether linkage when a polyester or a polyether soft segment is present may also act as a proton acceptor. Therefore, hydrogen bonding between hard segment–hard segment or hard segment–soft segment can exist. These bands have been widely used to characterize, at least semiquantitatively, the hydrogen bonding state of the polymer and to correlate this to the phase separation in the system. It is well known that in Hbonded urethane N-H and C=O bands appear at lower wavenumbers than that in free ones.[25] Figure 2 shows the FTIR spectra of C=O and N-H stretching vibration regions for synthesized polyurethanes. The band at 1740 cm^{-1} is ascribed to C=O stretching of the LDI and the remaining methyl ester groups of the polyether polyol, the broad band between 1730 and 1680 cm^{-1} is attributable to associated and nonassociated C=O urethane groups, and the small shoulders at 1663 and 1643 cm^{-1} are ascribed to associated and nonassociated urea linkages, which may be obtained from the reaction of some of the unreacted isocyanates with the atmospheric moisture while curing as a side reaction.

Analysis of amide-I stretching vibration for PU sample indicates that there is a band at approximately 1720 cm^{-1}, attributable to free C=O urethane groups, and a shoulder at about 1700 cm^{-1}, which is due to the H-bonded urethane.

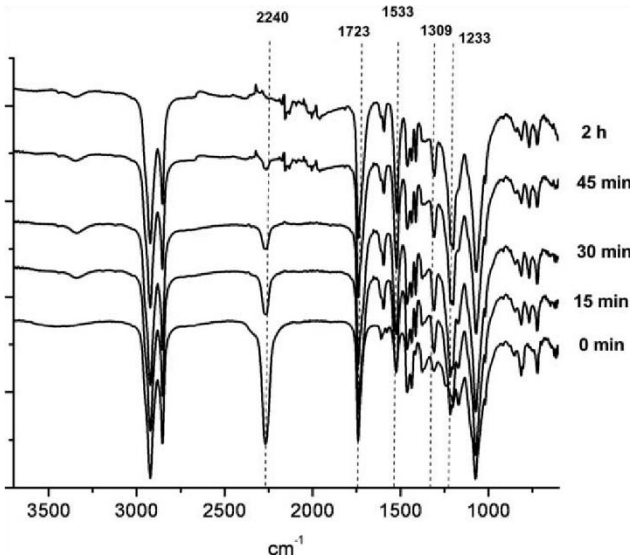

FIGURE 1 FTIR spectra of curing of PUM28.

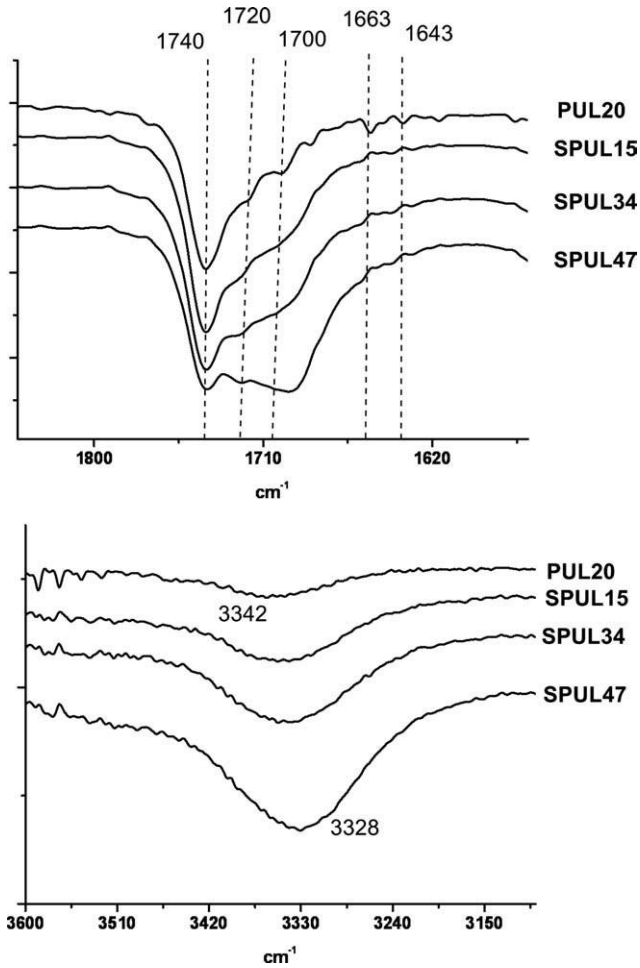

FIGURE 2 FTIR spectra of carbonyl (top) and amine (bottom) regions of polyurethanes.

The intensity of the bands attributed to free and H-bonded urethane carbonyls increases with increasing PDO fraction, as could be expected, because increasing PDO fraction leads to increased urethane content. The intensity of the band attributed to H-bonded urethane, relative to the band attributed to the nonbonded urethane groups, increases with an increase in the hard segment content. This suggests that the SPUL34 and SPUL47 C=O urethane groups are hydrogenbonded to a greater degree than the PUL20 and SPUL15 samples. In the amine region, the broad band ascribed to N-H stretching grows with the increase in urethane group concentration and shifts slightly to a lower wavenumber with increasing hard segment content, indicating an increase in the degree of association.

Thermal analysis of the polyurethanes was performed to provide insights into the morphological structure of the material. Thermal transitions are listed in Table 3 and Figure 3 shows the DSC thermograms for the segmented polyurethanes. For both series of nonsegmented polyurethanes, it was observed the expected trend: the T_g is higher when the functionality of the polyol is higher according to a higher degree of crosslinking. Moreover, differences can be observed for both isocyanates; the aromatic MDI leads to materials with higher T_g values than the aliphatic LDI. DSC thermograms of polyurethanes POH20/LDI extended with PDO showed an endothermic step in the heat flow at low temperatures, whereas in MDI-containing samples it could not be observed. Such transitions appeared in the region of 15 to 13 ^{o}C and were attributed to the POH soft-segment glasstransition temperature. This value is a measure of relative purity of the soft-segment regions; when there are hard segments dispersed in the soft domains, the T_g of the soft segment is raised. The degree of hard segment mixing into the soft-segment domain will depend on the overall hard segment content and the affinity of one segment toward the other. In our polyurethanes, hard segment content is high enough to achieve phase separation, and the experimental results revealed that the dispersion of hard segments in the soft domains seems to be low for LDI-containing polyurethanes. The results also show that the dispersion of the hard segments in the soft domain seems not to increase with the hard segment content.

Hard segment glass transition was observed at approximately 53–56 °C and 40–50 °C for SPUM and SPUL, respectively. Glass-transition temperatures for the hard segment depend strongly on its chemical structure and its molecular weight; it can therefore be stated that the lower hard segment T_g value in the SPUL samples could be a consequence of the irregular aliphatic structure of LDI.

No melting or crystallization peaks were found by DSC for the nonsegmented polyurethanes and for the LDI-containing segmented polyurethanes, according to the structure of amorphous materials. For the MDI-containing segmented polyurethanes, the most notable result of incorporating PDO is the appearance of melting endotherms of variable enthalpy and position, indicative of a semicrystalline structure. Melting behavior was complex, which can be attributed to a distribution of crystallite sizes or to the presence of different crystal forms. However, it seems that the nonsymmetrical diisocyanate LDI, which contains methyl ester side chain, produces hard segments that are unable to pack efficiently to form a crystalline hard segment domain.

TGA is the most favored technique for evaluation of the thermal stability of polymers. Polyurethanes have relatively low thermal stability, mainly due to the presence of urethane bonds. The thermal stability of the obtained polyurethanes was studied with TGA at a heating rate of 10 °C/min in nitrogen atmosphere, and the obtained data are shown in Table 3. The shapes of the weight loss curves of nonsegmented polyurethanes are almost identical, and differences in thermal stability seem to be small. It can be seen that the decomposition of the polyurethanes in nitrogen atmosphere does not take place below 330 °C.

The thermal decomposition of segmented polyurethanes involves at least two overlapping steps: a small drop below 300 °C is followed by the main loss weight above 300 °C (Fig. 4). The first weight loss is related to the decomposition of urethane bonds, which takes place through the dissociation to isocyanate and alcohol, the formation of primary amines and olefins, or the formation of secondary amines.[26] The main decomposition process is attributed to the polyether polyol chain scission and occurs at about 410 °C. The weight loss in the first step increases as the hard segment content increases, which is in accordance with the existence of a higher amount of weaker urethane bonds.

TABLE 3 Thermal and Mechanical Properties of the Polyurethanes

	T_g (°C)		TGA (N_2)				
Polyurethane	$1/2\ \Delta C_p$	tan δ_{max}	$T_{5\%\ loss}$ (°C)[a]	T_{max} (°C)[b]	Young's Modulus (MPa)	Tensile Strength (MPa)	Elongation (%)
PUM11	−29	−3	349	390	–	–	–
PUM15	−15	4	350	388	1.0	0.13	15
PUM20	−10	12	352	388	1.8	0.23	22
PUM28	9	23	350	392	3.5	0.20	13
PUM40	49	57	337	410	9.5	0.38	6
PUL11	−25	−10	352	392	–	–	–
PUL15	−21	−4	352	392	0.8	0.06	9
PUL20	−16	0	348	390	1.4	0.07	11
PUL28	−9	4	351	391	2.5	0.12	8
PUL40	23	29	343	412	6.0	0.18	5
SPUM15	−8, 55	26	316	321, 397, 459	7.0	0.60	14
SPUM34	56	25	302	306, 408, 464	30	1.80	10
SPUM47	53	24	295	303, 405, 469	74	3.10	10
SPUL15	−14	13, 81	307	304, 409	1.4	0.09	13
SPUL34	−13, 51	18, 77	292	303, 417	1.8	0.13	9
SPUL47	−15, 40	19, 77	281	296, 414	–	–	–

[a] Temperature of the 5% weight loss.

[b] Temperature of the maximum weight loss rate

The dynamic mechanical properties of the polyurethanes were obtained as a function of temperature beginning in the glassy state, through the T_g, and well into rubbery plateau of each material. Figure 5 shows the temperature dependence of the storage modulus and tan δ of the nonsegmented polyurethanes PUM and PUL. From the DMTA curves, the plateau of the elastic modulus in the rubbery state can be used to make qualitative comparisons of the level of cross-linking among the various polymers. Figure 5 shows that the value of the storage modulus in the rubber plateau increased, as the hydroxyl content of the starting polyol increased. DMTA also makes it possible to determine the T_g of the cross-linked materials. The T_g values determined by DMTA as the maximum of tan d are shown in Table 3. As expected, the T_g value is higher than the $1/2\Delta C_p$ from DSC, which can be related to the heat transporting hysteresis for large-scale samples in DMTA, and increase with increasing the hydroxyl content of starting polyol (Fig. 5). This is caused by the higher cross-linking degree, which increases the stiffness of the network structure.

Figure 6 shows the DMTA curves of segmented polyurethanes. In the glassy region, the storage moduli E′ is higher when the hard segment content is higher because of the increased number of urethane connections and the increase in interchain interactions caused by the hydrogen bonds. It seems that the hard segments play the role of physical cross-links and fillers, and this effect is more pronounced for MDI-containing polyurethanes than for LDI-containing polyurethanes. Figure 6 also shows the dissipation factor tan d curves as a function of temperature. Although DSC does not show the glass transition of the soft segment of MDI containing polyurethanes, it was clearly visible in DMTA experiments. Reference sample shows a tan d peak at 12 ^{o}C for PUM20 assigned to the glass transition of the amorphous soft segment. This peak shows a shift of maxima, decreasing height, and a broadening of the transition region as the hard segment content increases. This suggests greater limitations on freedom of chain mobility in the soft segment, which may be explained by the phase mixing between hard and soft segments. Although the tan d curves of SPUM polyurethanes show a unique transition, SPUL samples display the glass transition of the soft segment and a distinct transition at higher temperatures, which can be attributed to the T_g of the phase-separated hard block segments of the polymer. This transition becomes more prominent when the hard segment content increases because of a more phase separated morphology. Moreover, all tan d curves show a low temperature transition (around 50 ^{o}C). The origin of this peak is not known, but it is generally attributed to the rotational motions of the dangling fatty acid chains.[13] This peak is larger in segmented polyurethanes than in the reference sample. This relaxation at similar temperature was observed in other polyurethanes from vegetable oil-based polyols.[14]

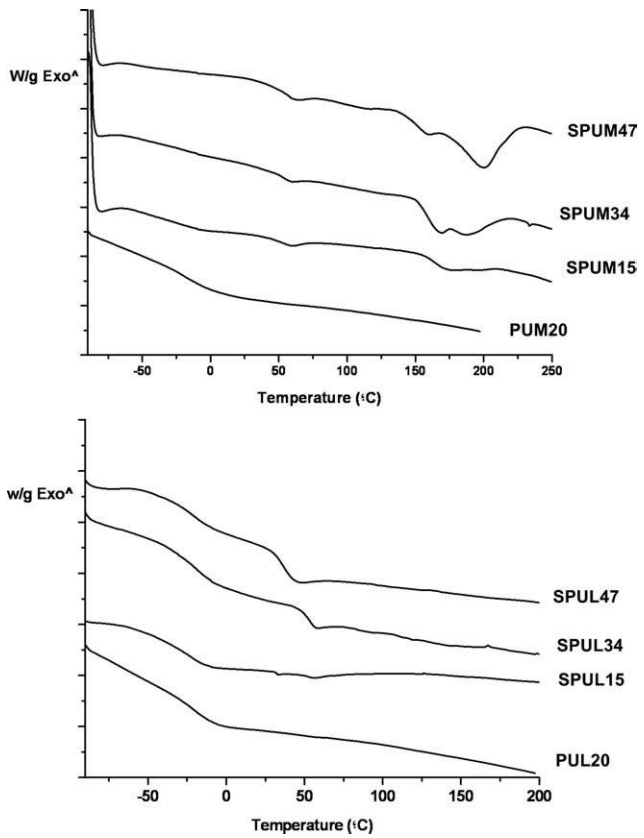

FIGURE 3 DSC thermograms (20 ^{o}C/min) of polyurethane networks.

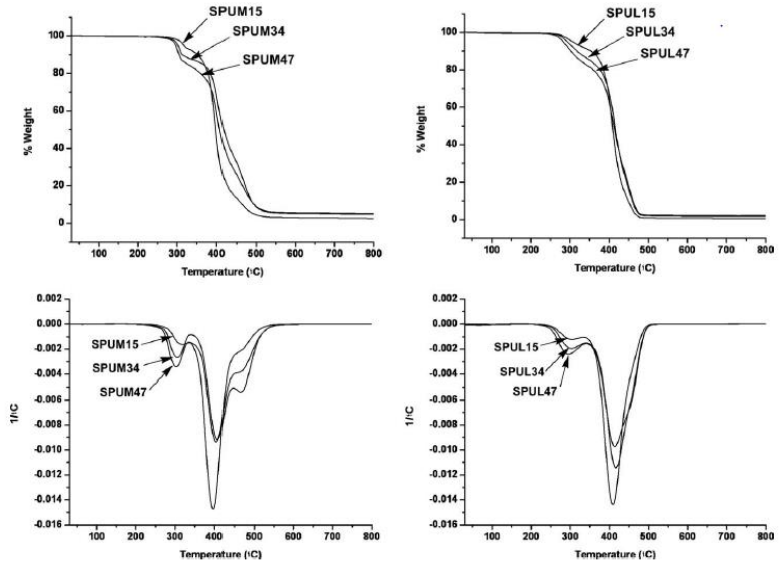

FIGURE 4 TGA plots (10 °C/min) and derivative curves of polyurethanes networks.

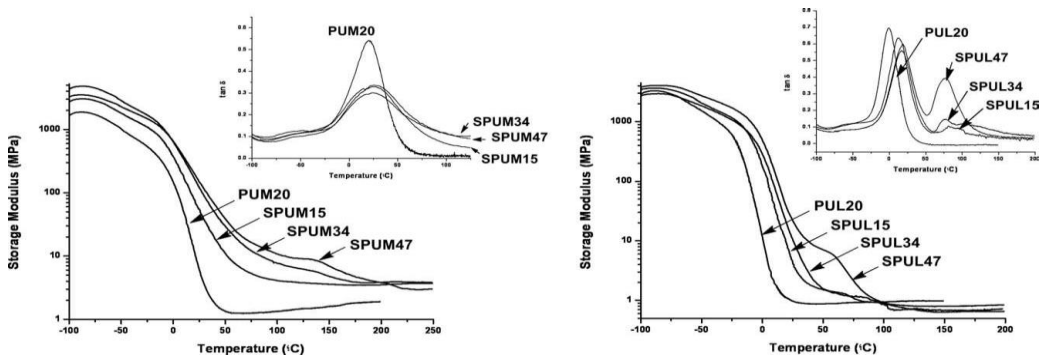

FIGURE 5 Storage modulus and loss factor of the nonsegmented polyurethanes.

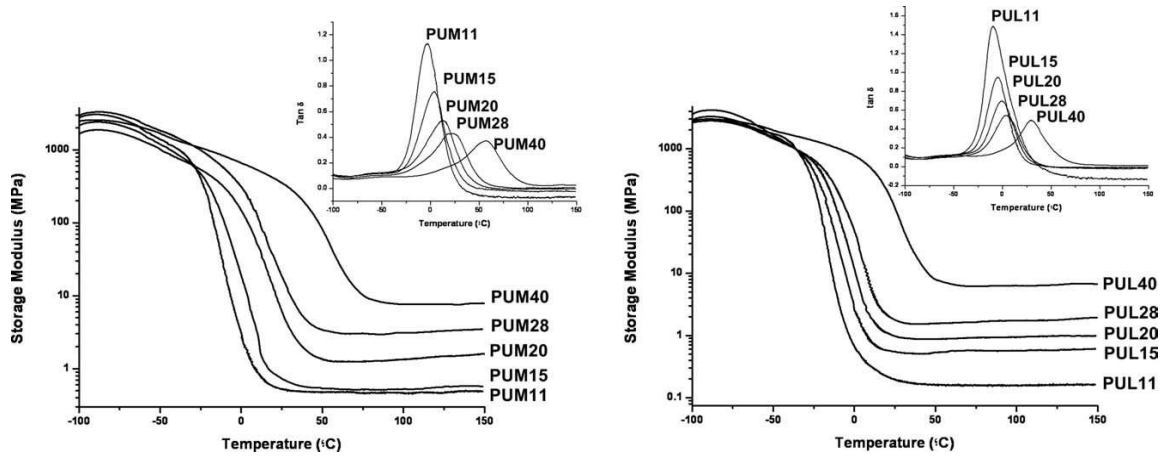

FIGURE 6 Storage modulus and loss factor of segmented polyurethanes.

Figure 7 shows the stress–strain curves of MDI-containing polyurethanes, and Table 3 summarizes the values of the mechanical properties of all the obtained polyurethanes. Young's modulus and tensile strength at break increase, whereas strain at break decreases in both segmented and nonsegmented polyurethanes, with increasing cross-linking density, which hinders molecular motion. The lower strength and modulus is a result of the higher amounts of dangling chains present, which are imperfections in the final polymer network and do not support stress when the network is under load. As expected, with increasing hard segment concentration, both Young's modulus and tensile strength increase. Finally, the use of the aliphatic diisocyanate LDI, which is weaker than aromatic diisocyanate MDI, limits the Young's modulus and tensile strength, specially for segmented polyurethanes.

As a conclusion, a variety of novel poly(ether urethane) networks were synthesized from polyether polyols obtained by ionic-coordinative polymerization of EMO. Nonsegmented polyurethanes show T_g values that increase as the functionality of the polyol increases and that are higher for the aromatic MDI than for the aliphatic LDI-containing materials. The segmented polyurethanes were phase segregated to varying degrees, and the use of nonsymmetric LDI inhibits hard segment crystallinity. All the polyurethanes are thermally stable over 300 ^{o}C, and their mechanical properties increase with increasing cross-linking density and hard segment concentration.

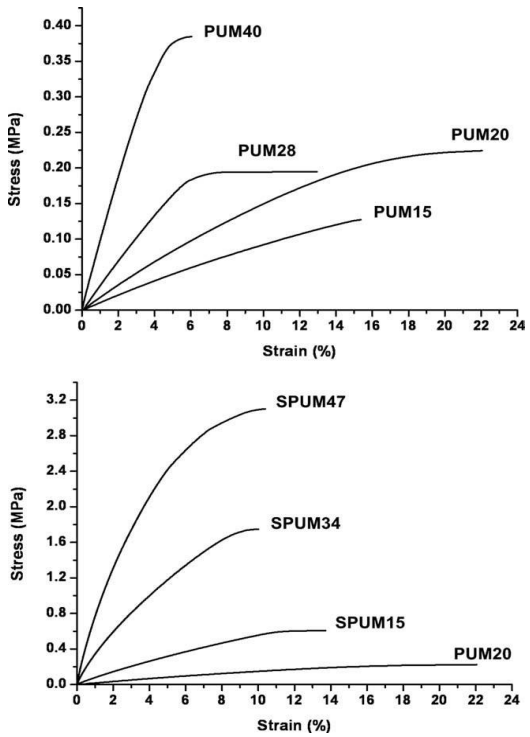

FIGURE 7 Stress–strain plots of the polyurethanes.

The authors acknowledge the financial support from MICINN (MAT2008-01412).

REFERENCES AND NOTES

1 (a) Raston, C. Green Chem 2005, 7, 57–57; 1 (b) Jenck, J. F.; Agterberg, F.; Droescher, M. J. Green Chem 2004, 6, 544–556.

2 Kaplan, D. L. Biopolymers from Renewable Resources; Springer: New York, 1998.

3 Belgacem, M. N.; Gandini, A. Monomers, Polymers and Composites from Renewable Resources; Elsevier: Oxford, 2008.

4 Meier, M. A. R.; Metzger, J. O.; Schubert, U. S. Chem Soc Rev 2007, 36, 1788–1802.

5 (a) Sharma, V.; Kundu, P. P. Prog Polym Sci 2008, 33, 1199–1215; (b) Sharma, V.; Kundu, P. P. Prog Polym Sci 2006, 31, 983–1008.

6 Guner, F. S.; Yagci, Y.; Erciyes, A. T. Prog Polym Sci 2006, 31, 633–670.

7 Lu, Y.; Larock, R. C. ChemSusChem 2009, 2, 136–147.

8 Szycher, M. Szycher's Handbook of Polyurethanes. CRC Press: Boca Raton, FL, 1999.

9 Petrovic, Z. S. Polymer Rev 2008, 48, 109–155.

10 Guo, A.; Cho, I. J.; Petrovic, S. J Polym Sci Part A: Polym Chem 2000, 38, 3900–3910.

11 Zlatanic, A.; Petrovic, Z. S.; Dusek, K. Biomacromolecules 2002, 3, 1048–1056.

12 Guo, A.; Demydov, D.; Zhang, W.; Petrovic, Z. S. J Polym Environ 2002, 10, 49–52.

13 Petrovic, Z.; Zhang, W.; Javni, I. Biomacromolecules 2005, 6, 713–719.

14 Lligadas, G.; Ronda, J. C.; Galia, M.; Biermann, U.; Metzger, J.O. J Polym Sci Part A: Polym Chem 2006, 44, 634–645.

15 Dietrich, D.; Uhlig, K. In Ullmann's Encyclopedia of Industrial Chemistry; Elvers, B.; Hawkins, S.; Schulz, G., Eds.; VCH: Weinheim, 1992.

16 Lligadas, G.; Ronda, J. C.; Galia, M; Cadiz, V. Biomacromolecules 2007, 8, 686–692.

17 Lligadas, G.; Ronda, J. C.; Galia, M; Cadiz, V. Biomacromolecules 2006, 7, 2420–2426.

18 Inoue, S.; Aida, T. In Polyethers; Handbook of Polymer Synthesis, Part A; Marcel Dekker: New York, 1991.

19 Ronda, J. C.; Serra, A.; Cadiz, V. Macromol Chem Phys 1999, 200, 221–230.

20 Muggee, J.; Vogl, O. J Polym Sci Polym Chem Ed 1985, 23, 649–671.

21 del Rio, E.; Galia, M.; Cadiz, V.; Lligadas, G.; Ronda, J. C. J Polym Sci Part A: Polym Chem, submitted for publication.

22 Venturello, C.; D'Aloisio, R. JOrgChem 1988, 53, 1553–1557.

23 Skrovanek, D. J.; Howe, S. E.; Painter, P. C.; Coleman, M. M. Macromolecules 1985, 18, 1676–1683.

24 Papadimtrakopoulos, F.; Sawa, E.; MacKnight, W. J. Macromolecules 1992, 25, 4682–4691.

25 Seymour, R. W.; Estes, G. M.; Cooper, S. L. Macromolecules 1970, 3, 579–583.

26 Levchik, S. V.; Weil, E. D. Polym Int 2004, 53, 1585–1610.